



Contents lists available at ScienceDirect

Journal of Human Evolution

journal homepage: www.elsevier.com/locate/jhevol

Episodes of environmental stability versus instability in Late Cenozoic lake records of Eastern Africa

Martin H. Trauth^{a,*}, Andreas G.N. Bergner^a, Verena Foerster^b, Annett Junginger^c,
Mark A. Maslin^{c,d}, Frank Schaebitz^b

^a Institute of Earth and Environmental Science, University of Potsdam, Karl-Liebknecht-Str. 24–25, 14476 Potsdam, Germany

^b Seminar of Geography and Education, University of Cologne, Gronewaldstraße 2, 50931 Köln, Germany

^c Senckenberg Center for Human Evolution and Palaeoenvironment, Department of Earth Sciences, University of Tübingen, Hölderlinstr. 12, 72074 Tübingen, Germany

^d Department of Geography, University College London, Pearson Building, Gower Street, London WC1H 0AP, UK

ARTICLE INFO

Article history:

Received 17 November 2013

Accepted 25 March 2015

Available online xxx

Keywords:

Paleoclimate

East Africa

Human evolution

Lakes

Sediments

ABSTRACT

Episodes of environmental stability and instability may be equally important for African hominin speciation, dispersal, and cultural innovation. Three examples of a change from stable to unstable environmental conditions are presented on three different time scales: (1) the Mid Holocene (MH) wet–dry transition in the Chew Bahir basin (Southern Ethiopian Rift; between 11 ka and 4 ka), (2) the MIS 5–4 transition in the Naivasha basin (Central Kenya Rift; between 160 ka and 50 ka), and (3) the Early Mid Pleistocene Transition (EMPT) in the Olorgesailie basin (Southern Kenya Rift; between 1.25 Ma and 0.4 Ma). A probabilistic age modeling technique is used to determine the timing of these transitions, taking into account possible abrupt changes in the sedimentation rate including episodes of no deposition (hiatuses). Interestingly, the stable-unstable conditions identified in the three records are always associated with an orbitally-induced decrease of insolation: the descending portion of the 800 kyr cycle during the EMPT, declining eccentricity after the 115 ka maximum at the MIS 5–4 transition, and after ~10 ka. This observation contributes to an evidence-based discussion of the possible mechanisms causing the switching between environmental stability and instability in Eastern Africa at three different orbital time scales (10,000 to 1,000,000 years) during the Cenozoic. This in turn may lead to great insights into the environmental changes occurring at the same time as hominin speciation, brain expansion, dispersal out of Africa, and cultural innovations and may provide key evidence to build new hypotheses regarding the causes of early human evolution.

© 2015 Elsevier Ltd. All rights reserved.

1. Introduction

The possible influence of environmental variability, both temporally and spatially, on human evolution and dispersal is an intensely debated topic in the scientific community (Potts, 1996; Trauth et al., 2005, 2007; Maslin and Christensen, 2007; Maslin and Trauth, 2009; Potts, 2013; Maslin et al., 2014). However, recent evidence indicates that episodes of stable environmental conditions play an equally important role for human evolution, dispersal, and technological innovation (e.g., Grove, 2013; Shultz and Maslin, 2013). Periods of reduced environmental variability

may encourage the growth of hominin populations, sympatric evolution, and dispersal, whereas episodes of less favorable conditions, pronounced droughts, or rapid shifts between wet and dry climates could result in geographical isolation and allopatric speciation (Maslin and Trauth, 2009).

The sedimentary record of Eastern African lakes is rich in examples of both environmental stability and instability in the course of climate change (e.g., Trauth et al., 2003, 2005; Foerster et al., 2012; Junginger and Trauth, 2013; Junginger et al., 2014; Fig. 1). These lakes, particularly those that occur in the rift basins, are amplifiers of moderate climate change (Olaka et al., 2010; Trauth et al., 2010). As an example, the water level of the Early Holocene paleo-Lake Suguta rose to 300 m during a +25% change in precipitation during the African Humid Period (ca. 15 ka–5 ka; Garcin et al., 2009; Borchardt and Trauth, 2012; Junginger and Trauth,

* Corresponding author.

E-mail address: trauth@geo.uni-potsdam.de (M.H. Trauth).

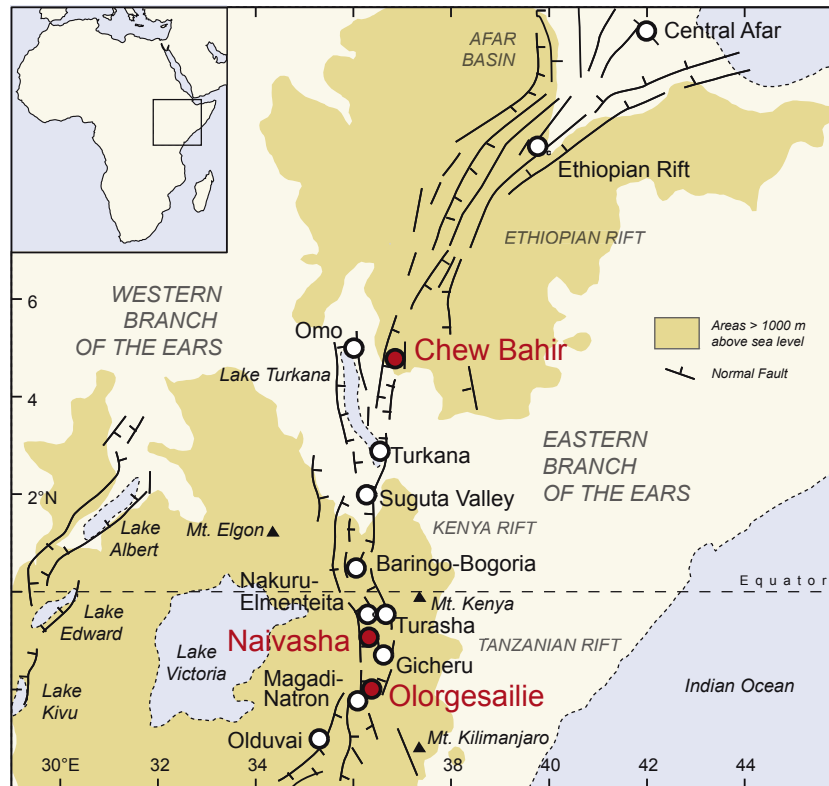


Figure 1. Map of Eastern Africa showing topography, faults, and lake basins. Note the location of the studied sites Chew Bahir, Naivasha and Olorgesailie (modified from Trauth et al., 2005).

2013). On the other hand, as hydrological modeling suggests, large water bodies buffer rapid shifts in climate due to their delayed response to changes in the precipitation–evaporation balance (Borchardt and Trauth, 2012). The identification and correlation of episodes of stability versus instability between lake basins, however, is unfortunately hampered by ambiguous interpretation of environmental indicators or proxies within the sediments (Owen et al., 2008, 2009; Trauth and Maslin, 2009). Furthermore, fluctuating sedimentation rates and hiatuses between radiometric age dates, which themselves contain errors, complicates the assessment of the actual timing of environmental stability versus instability (e.g., Sadler, 1999; Blaauw, 2010; Schumer and Jerolmack, 2009; Trauth, 2014).

This manuscript attempts to meet this challenge and presents three examples of stability versus instability on three different time scales in lake records in Eastern Africa: (1) the Mid Holocene (MH) wet–dry transition in the Chew Bahir basin (Southern Ethiopian Rift; between 11 ka and 4 ka), (2) the MIS 5–4 transition in the Naivasha basin (Central Kenya Rift; between 160 ka and 50 ka), and (3) the Early Mid Pleistocene Transition (EMPT) in the Olorgesailie basin (Southern Kenya Rift) (between 1.25 Ma and 0.4 Ma). First, we re-analyze the three lake records using a probabilistic technique to determine the best age model for stratigraphic sequences (Trauth, 2014). Second, we interpolate the published lake records on the new age model and distinguish episodes of environmental stability versus instability in the records. Third, we put together plausible mechanisms that cause stable or unstable conditions in the course of climate change. Last, the results are discussed in light of the importance of both stability and instability for human evolution and dispersal, providing a basis for further discussions of the influence of the environment on early humans.

2. Detecting episodes of stability and instability in lake records

In our analysis of episodes of environmental stability and instability, we use published lake records, which include critical episodes of Eastern African climate change and human evolution, dispersal, and cultural innovation. We use the amplitudes of water level changes as published, without revising or reinterpreting the proxies of lake levels and climate used by the authors of the original works. While the amplitudes have been left untouched, we have subjected all age models to a critical review because the timing and rate of climate change as well as its correlation with orbital forcing is essential for our analysis. Having developed consistent age models for the three records, we defined episodes of relative stability and instability by visual inspection and correlated these with orbital forcing (Laskar et al., 2004). We have not used any more sophisticated method to determine the degree of variability for two reasons: (1) the quantitative significance of the records is not sufficient to analyze them statistically, and (2) an arbitrary definition of a critical value of the variability would be necessary to separate stable from unstable episodes, which we wanted to avoid.

2.1. The Mid Holocene (MH) wet–dry transition in the Chew Bahir basin

The Mid Holocene (MH) wet–dry transition in the Chew Bahir basin (Southern Ethiopian Rift) is reconstructed from five up to ~20 m long sediment cores (CB01, CB03–06) collected along a ~20 km long NW–SE transect across the basin (Foerster et al., 2012, 2014). The composite age model of the sediment cores is based on 32 AMS ^{14}C ages derived from biogenic carbonate, fossilized

charcoal, and organic sediment, resulting in a statistically robust chronology for lake record spanning the last 45 ka (Foerster et al., 2012; Fig. 2A).

The proxy-climate record of the Chew Bahir basin is based on potassium (K^+) abundance, previously established as a reliable proxy for aridity in the Chew Bahir cores (Foerster et al., 2012). The potassium (K^+) record of cores CB03–06 has been tuned to the K^+ record of CB01 assuming that K^+ , as a weathering product of feldspar, feldsparoids, and mica, is transported instantaneously in solution from source to sink, and complete mixing in the water body of paleo-Lake Chew Bahir. We used linear and cubic spline interpolation techniques while tuning the individual records, but we have found no significant difference in the final result. All radiocarbon ages were converted into calibrated ages with OxCAL using the IntCal13 calibration curves (Bronk Ramsey, 1995, 2009a,b; Reimer et al., 2013). The best estimate of the true age was obtained

by calculating the weighted mean of the probability density function of the calibrated ages.

The potassium and all other proxy records were interpolated upon the age model using a linear interpolation technique. We prefer a linear over a spline model as abrupt variations between low or high sedimentation rates, even episodes without deposition, may actually exist in rift basins; these are smoothed out by splines and age modeling techniques introducing an arbitrarily chosen memory (e.g., Bronk Ramsey, 2008, 2009a,b; Blaauw and Christen, 2011; Trauth, 2014). We used the K^+ record between 11 and 4 ka of core CB01 for our analysis of stability versus instability because it is the most complete and detailed record of the Mid Holocene (MH) wet–dry transition in the Chew Bahir basin. Between ~9.8 ka and 9.1 ka we fill a gap in the core CB01 with the corresponding piece from the adjacent core CB03.

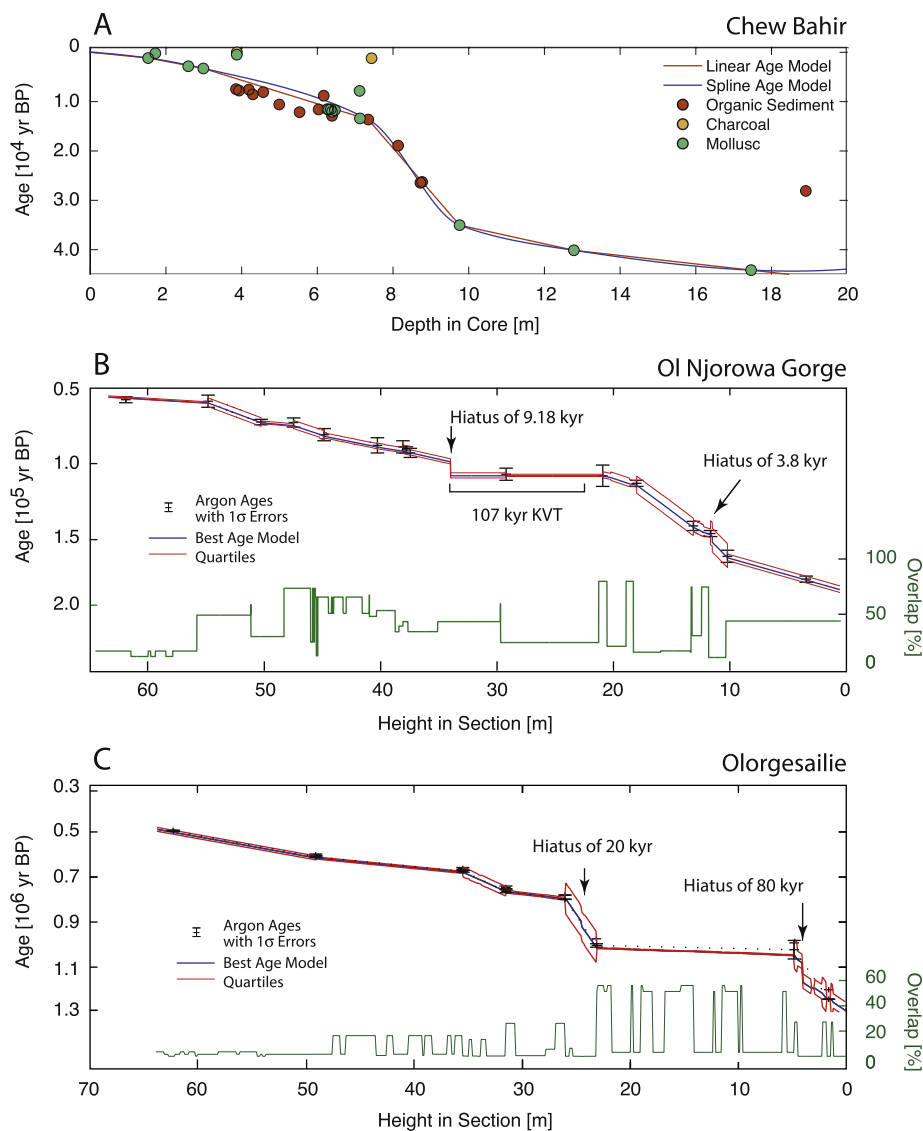


Figure 2. Age models of three studied records. (A) The composite age model of the Chew Bahir basin is based on 32 AMS ¹⁴C ages (Foerster et al., 2012, 2014). All radiocarbon ages were converted into calibrated ages with OxCAL using the IntCal13 calibration curves (Bronk Ramsey, 1995, 2009a,b; Reimer et al., 2013). The best estimate of the true age was obtained by calculating the weighted mean of the probability density function of the calibrated ages. (B) and (C) The age model of the Naivasha and Olorgesailie records was calculated using a probabilistic technique for complex stratigraphic sequences simply comparing the deposition time of equally thick sediment slices from the differences of subsequent radiometric age dates and the unit deposition times (the inverse of the sedimentation rate) of the various sediment types (Trauth, 2014).

2.2. The MIS 5–4 transition in the Naivasha basin

The MIS 5–4 transition is recorded in the 60 m thick Ol Njorowa Gorge section in the southern Naivasha basin, which covers the interval between ~150 ka and 60 ka (Trauth et al., 2001, 2003). The age model is based on anorthoclase and sanidine phenocryst concentrates from 16 tephra beds dated by the laser-fusion $^{40}\text{Ar}/^{39}\text{Ar}$ method (Trauth et al., 2001, 2003). The lake record has been inferred from sediment characteristics, diatoms, and authigenic mineral assemblages (Trauth et al., 2001, 2003). The best age model was determined using a technique presented by Trauth (2014). In contrast to established age modeling techniques, such as intuitive definition of the age–depth relationship, calibrating the stratigraphy to insolation or orbital target curves, Monte-Carlo modeling of age distributions along sediment cores, and Bayesian age–depth models (see review of Blaauw, 2010; Trauth, 2014), the approach by Trauth (2014) helps detect abrupt variations in sedimentation rates, including the possibility of episodes of no deposition (hiatuses).

The new probabilistic technique for complex stratigraphic sequences simply compares the deposition time of equally thick sediment slices from the differences of subsequent radiometric age dates and the unit deposition times (the inverse of the sedimentation rate) of the various sediment types. First, the time difference is determined from the two $^{40}\text{Ar}/^{39}\text{Ar}$ dates and their independent Gaussian errors. Second, the time difference is again calculated from the unit deposition time of the sediment types and their Gamma-distributed dispersion (Trauth, 2014). The percentage overlap of the distributions of these two sources of information, together with the evidence from the sedimentary record, helps to find the best age model of complex sequences including abrupt variations in the rate of deposition incorporating one or more hiatuses.

The sedimentation rates of the various types of deposits exposed in the Ol Njorowa Gorge are very different, ranging from less than a tenth of a millimeter per year for diatomite to several meters of volcanic airfall deposits within a couple of hours, followed by a longer period of time with no deposition (Trauth et al., 2001, 2003). Most importantly, a thick welded tuff called the Kedong Valley Tuff, 106 ± 4 ka, is located in the middle of the section, which is considered to be deposited within zero time on the $^{40}\text{Ar}/^{39}\text{Ar}$ time scale. The chronology is free of age reversals within the one-sigma error bars of the argon ages. The means, however, show in fact two reversals at the top (61.9 m, 60 ± 2 ka) and in the middle of the section (40.28 m, 92 ± 5 ka). Statistical age modeling requires monotonically increasing ages from top to bottom of the section (e.g., Blaauw and Christen, 2011; Trauth, 2014). Therefore, we have edited the age of these two layers within the error bars of the $^{40}\text{Ar}/^{39}\text{Ar}$ ages: 58 ka and 88 ka. This is quite permissible within the error bars, particularly since the modification of the ages does not affect the modeling result.

The Gamma model for the most likely unit deposition time for each sediment type (e.g., three types of materials: tephra, clastic sediments, diatomite) has two parameters: shape and scale. In the experiments described here, a Gamma model gamma with shape = 2 best describes the frequency distribution of unit deposition times, which is in agreement with the work of Blaauw and Christen (2011). We used a scale factor of 1.5, 2.0, and 8.0 for the three sediment types: tephra, clastic sediments, and diatomite. A first run of the model was used to adjust the Gamma parameters for the corresponding to sedimentation rates of ~0.667, 0.500, and 0.125 mm/yr.

2.3. The Early Mid Pleistocene transition in the Ologesailie basin

The EMPT is recorded in the 80 m thick Ologesailie Formation exposed in the Ologesailie basin, which covers the interval between ~1.25 Ma and 0.49 Ma (Deino and Potts, 1990; Behrensmeier

et al., 2002; Owen et al., 2008, 2011; Deocampo et al., 2010). The age model is based on seven $^{40}\text{Ar}/^{39}\text{Ar}$ ages of tephra layers, of which neither the oldest date (1.20 Ma) nor the ~780 ka Bruhnes-Matuyama magnetic reversal has an error bar (Deino and Potts, 1990; Behrensmeier et al., 2002; Owen et al., 2008, 2011; Deocampo et al., 2010). Again, we used the new probabilistic technique for complex stratigraphic sequences by Trauth (2014) to determine the best age model of the Ologesailie sequence. The lake record is taken from Figure 4 of Behrensmeier et al. (2002), describing three different environments: (1) fluctuating lacustrine, (2) wetland, and (3) subaerial conditions.

Behrensmeier et al. (2002) classify the sediment layers of the Ologesailie formation in four types of deposits: (1) sands and/or gravel, (2) subaerial exposure, (3) extensive pedogenesis, and (4) bedded diatomite. We interpret these types of deposits as (1) coarse-grained sediments, (2) and (3) fine-grained sediments of two different types, and (4) diatomite, where the precise distinction is not decisive for the outcome of the experiment. Interactive modeling yields a Gamma model for the sediment types with a shape factor of 2 and scale factors of 0.5 for coarse-grained sediments, 2 for both types of fine-grained sediments (although the model also allows for different values), and 20 for diatomite. The corresponding sedimentation rates are 2 mm/yr for coarse-grained sediments, 0.5 mm/yr for fine-grained deposits, and 0.05 mm/yr for diatomite.

3. Examples for stability–instability in Cenozoic lake records

3.1. The stability–instability transition in the Mid Holocene Chew Bahir record

Although we are interested only in the time interval between 11 ka and 4 ka, a consistent age model for the entire core using all AMS ^{14}C ages must be calculated (Foerster et al., 2012, 2014; Fig. 2A). In a first approximation, the age model based on radiocarbon dating of mixed materials suggests a linear relationship between age and depth, with a two-time change in the sedimentation rate at ~9.75 m and 7.35 m (Foerster et al., 2012, 2014; Fig. 2A). The timing of the transitions correlates with a change of climate in Eastern Africa. Two wet episodes before 35 ka and after ~15 ka (the so-called African Humid Period, between ~15 ka and 5 ka; e.g., Barker et al., 2004) with sedimentation rates in the order of ~0.5–0.6 mm/yr are bracketing an episode of a drier climate during the Last Glacial Maximum with sedimentation rates of ~0.1 mm/yr (Foerster et al., 2012, 2014). The sedimentation rates vary not only with time but also from core to core along the transect of the pre-study. The mean sedimentation rate (SAR) decreases from ~0.7 mm/yr at the basin margin (core CB01) to ~0.2 mm/yr towards the center (CB05; Foerster et al., 2012, 2014). A closer look at the age model reveals slightly too old radiocarbon ages between 6.5 m and 3.0 m composite depth, i.e., slightly delayed by ~1.0 m compared with the African Humid Period (~7.5–4.0 m composite depth), suggesting temporary storage and remobilization of organic matter in the densely vegetated catchment during a wetter climate (Fig. 2A). Three ages, younger than 2 ka, at ~7.45 m and 3.9 m, are believed to be too young due to contamination of the sediment core (Foerster et al., 2012, 2014; Fig. 2A).

The examination of the K+ record between 11 ka and 4 ka reveals an episode of relative environmental stability until about 8.2 ka, before a distinctive drought event occurs at ~8.15 ka (Fig. 3A). This drought event is the first of a series of five events, between ~40 and 80 years long, each of which is documented by two to six data points in our K+ record. An episode of relative instability, characterized by a relatively wet climate with a decrease in humidity between ~8.15 ka and 7.75 ka and interrupted by the

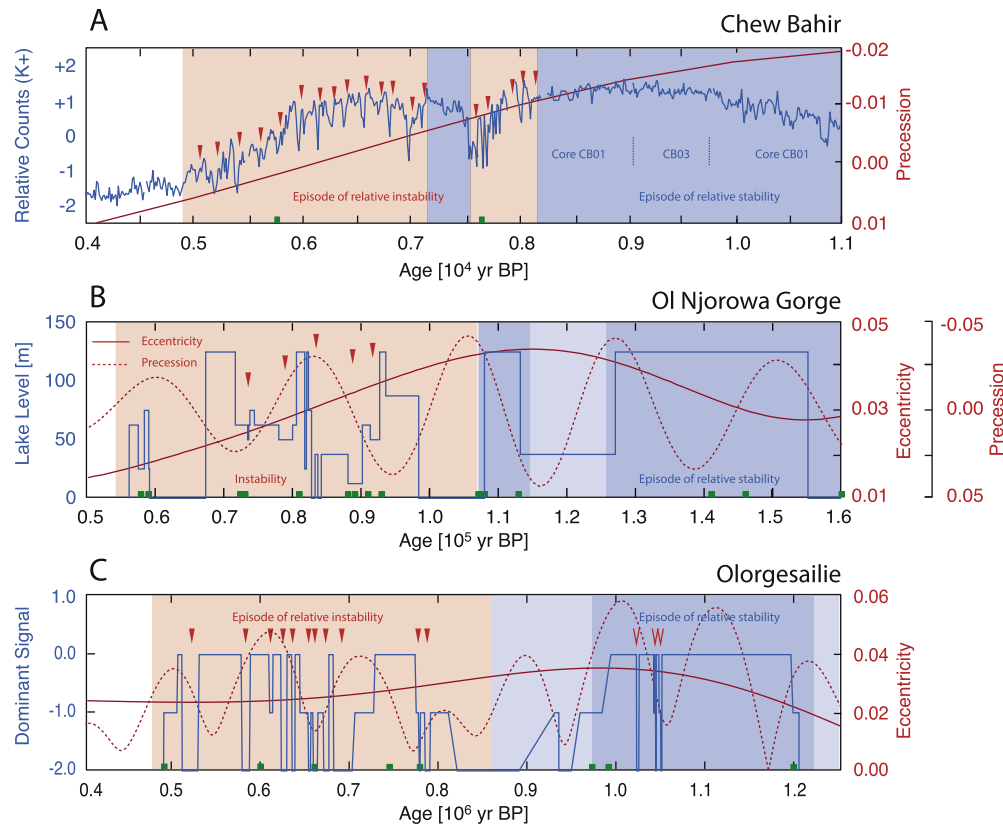


Figure 3. Lake level records of the three studied sites (blue lines) with age control points (green squares) and orbital and precessional quantities (red lines) to define episodes of relative stability and instability with pronounced dry periods (red triangles). (A) Holocene environmental record of the Chew Bahir basin created by tuning the potassium records of five cores (CB01 and CB03–06) and interpolating the record to the age model shown in Figure 2A. (B) Late Pleistocene lake-level record of Lake Naivasha obtained by recalibrating the record published in Trauth et al. (2001, 2003) to the new age model shown in Figure 2B. (C) Mid Pleistocene record of the Ologesailie basin taken from Behrensmeier et al. (2002), re-calibrated to the revised age model shown in Figure 2C and plotted together with the earth's eccentricity cycle (solid red line) as well as its 800 kyr component (dashed red line). All orbital and precessional quantities taken from Laskar et al. (2004). (For interpretation of the references to colour in this figure legend, the reader is referred to the web version of this article.)

~80–40 year long drought events, is followed by an interval of relative stability between ~7.75 ka and 7.15 ka at a high moisture level. This wet and stable episode is again followed by a two-thousand year long interval of instability between ~7.15 ka and 5 ka. The episode of relative stability is characterized by a relatively high moisture level between ~7.15 ka and 5.95 ka, before the onset of one-thousand year long drying of the region. The entire period between ~7.15 ka and 5 ka is again characterized by at least fourteen pronounced drought events, again between ~20 and 80 years long, each of which is documented by two to seven data points in our K+ record. This unstable interval is followed by relatively dry and stable climate after ~5 ka.

In a first approximation, the K+ record follows the earth's precession cycle during the interval from 11 ka to 4 ka, which is in agreement with the proposed link between increased humidity during the African Humid Period (AHP) and more intense heating of the northern hemisphere as a consequence of a minimum in the orbital precession (e.g., Kutzbach and Liu, 1997; Fig. 3A). On closer inspection, however, the K+ record suggests a strong nonlinear relationship between orbital forcing and climate during the Mid Holocene (MH) wet–dry transition in the Chew Bahir basin and its catchment. During the precession increase from -0.020 to zero, the climate on average between 11 ka and 4 ka remained relatively moist. However, after falling below zero, the climate became unstable with pronounced dry periods recurring every 160 ± 40 years, which have a duration of 80–20 years. When the precession increased above $+0.005$, climate returned to relative stability, but at a much lower moisture level.

3.2. The stability–instability transition in the Late Pleistocene Naivasha record

We examine the period between 160 ka and 50 ka, for which we calculate the most likely age model (Fig. 2B). First, we have calculated an age model based on the unit deposition times of the three types of sediments: tephra, clastic sediments, and diatomite. The determination of the best age model requires the interactive adjustment of the age of the base of the section and the Gamma parameters of each sediment type. Using an age of 183 ka for the base of the section and the scale factors of 1.5, 2.0, and 8.0 for the three sediment types of tephra, clastic sediments, and diatomite, corresponding to sedimentation rates of ~0.667, 0.500, and 0.125 mm/yr, respectively, leads to the best fit between the age model and the independent argon ages of the section.

Second, we compare the unit deposition times (and their Gamma distributions) with the differences of subsequent radiometric age dates (and their Gaussian distributions). The percentage overlaps of the distributions ranges from 11 to 80%, with the lower values indicating possible abrupt changes in the sedimentation including episodes of no deposition (hiatuses; Fig. 2B). Using this information we find a hiatus at 11.5 m height in the section, where we add 3.8 kyrs to the age model. At this location in the section, the percentage overlap between the two sources of evidence, the sediment types and argon ages, is only ~11%. Introducing an interval of 3.8 kyr without deposition causes a perfect match between the age model and the argon ages in this part of the section. If we examine the stratigraphic description of the 0.12 m thick unit in the

profile, which includes the possible hiatus, we find a complex deposit comprising sands and silts, mixed with diatomaceous sediments, but also volcanoclastic deposits with rounded pumice lapilli and rock fragments (Trauth et al., 2001, 2003). This unit is immediately below the oldest diatomite unit, 3.30 m thick, documenting a major lacustrine interval in the Naivasha basin.

A second hiatus is possibly located at 34 m just above the Kedong Valley Tuff, 106 ± 4 ka, located in the middle of the section, which is considered to be deposited within zero time on the $^{40}\text{Ar}/^{39}\text{Ar}$ time scale. The best match between the age model and the argon ages is obtained by introducing an interval of no deposition with a duration of 9.18 kyrs at the top of the tuff. Again, the examination of the stratigraphic log of the section reveals a 0.3 m thick unit of a sandy tuff overlying the heavily eroded and weathered top of the Kedong Valley Tuff, suggesting subaerial conditions after the deposition of the 10 m thick tuff in a shallow lake in the southernmost part of the Naivasha basin (Trauth et al., 2001, 2003). At this location in the section, the percentage overlap between the two sources of evidence, the sediment types and argon ages, is only ~43%.

The Late Pleistocene lake level record from the Naivasha basin reveals a relatively long episode of stability between 155 ka and 106 ka, which is particularly evident through a series of diatomite beds with a total thickness of ~4.9 m with intercalated clastic and volcanoclastic deposits (Fig. 3B; Trauth et al., 2001, 2003). During this lake episode, the lake has reached water depths of up to 150 m and a size of ~520 km², whereas the up to 9 m deep modern lake covers only ~180 km² (Bergner et al., 2003). Climate variability during this interval was relatively low, as pH fluctuations between ~8.0 and 8.5 of the lake water inferred from diatom assemblages suggest (Bergner and Trauth, 2004). In contrast, the episode after ~106 ka is characterized by remarkable climate fluctuations (Trauth et al., 2001, 2003). Short freshwater phases are characterized by thin diatomite layers, unaltered volcanic glass, and absence of authigenic silicates. In contrast, silicic glass with perlitic cracks, glass shards with montmorillonite rims, occasional chabazite, and phillipsite represent the transition to alkaline conditions with a pH of about 9. Even higher alkalinity results in the formation of clinoptilolite, and extremely alkaline pore waters (pH > 11) lead to the precipitation of analcime (Trauth et al., 2001, 2003). The diatomite layers within this part of the section are characterized by diatom species with a preference for slightly higher alkalinities than the ones identified in the lower, thick diatomite beds (Bergner and Trauth, 2004).

The relation between climate and orbital forcing is complex in this part of Eastern Africa, as it seems to follow equatorial March and September insolation at times of maximum eccentricity and hence maximum amplitude of the Earth's precessional cycle, causing half precessional cycles (~11.5 kyr) rather than precessional (~23 kyr) in climate records (Berger and Loutre, 1997; Trauth et al., 2003; Berger et al., 2006). Furthermore, it seems the complex topography of the East African Rift System, with its horst and graben structures and extensive plateaus, modulates this influence in a complicated manner (Trauth et al., 2010). The new age model of this section suggests lake highstands as the result of a wetter climate between 155 ka and 127 ka, 113 ka and 108 ka, as well as between ~98 ka and 93 ka, ~83 ka and 80 ka, and ~72 ka and 67 ka, which is slightly different from the chronology of high lake levels as published by Trauth et al. (2001, 2003). Whereas the old chronology of highstands suggests a linear correlation of the lake level with March and September insolation, the lake record according to the new age model suggests a more complex link between insolation and the hydrological budget of Lake Naivasha than previously thought. The lake highstands, however, seem to occur 5000–2000 years after minimum or maximum precession, suggesting a causal

but complex link between orbital forcing and humidity between 160 ka and 50 ka (Fig. 3B). Between these wet episodes, the most remarkable drought events are centered at ~91, 88, 83, 78, and 73 ka (i.e., within the episode of instability after ~106 ka; Fig. 3B).

3.3. The stability–instability transition in the Early Mid Pleistocene Olorgesailie record

The Early to Mid Pleistocene lake sediment sequence exposed in the Olorgesailie basin has led to lively discussions during the last couple of years (Trauth and Maslin, 2009; Owen et al., 2009). In particular, there is disagreement over the duration of stable lacustrine conditions, which is documented in up to 7 m thick diatomite beds within the section. In our interpretation of the published evidence by Behrensmeier et al. (2002), we concluded that a large, deep lake existed between ~1.2 Ma and 0.9 Ma, whereas Owen et al. (2009) read the same stratigraphic section as the record of a series of short (less than 10 ka) lacustrine episodes, interrupted by long (more than 200 kyr) intervals of complex conditions including several hiatuses (Owen et al., 2009). According to the interpretation of Owen et al. (2009), only ~45% of the time interval between ~1.25 Ma and 0.49 Ma is recorded in the sediments of the Olorgesailie formation. On the other hand, the Olorgesailie formation is the key section for the variability selection hypothesis by Potts (1996) claiming that environmental instability is a key driver of evolution.

We examined the period between 1.25 Ma and 0.49 Ma, for which we calculated the most likely age model (Fig. 2C) using the approach by Trauth (2014). First, we calculated an age model based on the unit deposition times of the four types of sediments: coarse-grained sediments, fine-grained sediments of two different types, and diatomite. The determination of the best age model requires the interactive adjustment of the age of the base of the section and the scale factors of 0.5 for coarse-grained sediments, 2 for both types of fine-grained sediments, and 20 for diatomite, corresponding to sedimentation rates of 2 mm/yr, 0.5 mm/yr, and 0.05 mm/yr, respectively, which leads to the best fit between the age model and the independent argon ages of the section.

Second, we compared the unit deposition times (and their Gamma distributions) with the differences of subsequent radiometric age dates (and their Gaussian distributions). The percentage overlaps of the distributions range from close to zero to ~56%, with the lower values indicating possible abrupt changes in the sedimentation including episodes of no deposition (hiatuses; Fig. 2C). Using this information we found a hiatus at 4.0 m height in the section, where we added 80 kyr to the age model. At this location in the section, the percentage overlap between the two sources of evidence, the sediment types and argon ages, is close to zero. Introducing an interval of 80 kyr without deposition causes a perfect match between the age model and the argon ages in this part of the section. A second hiatus is possibly located at 24.5 m. The best match between the age model and the argon ages is obtained by introducing an interval of no deposition with a duration of 20 kyr at the top at this level. At this location in the section, the percentage overlap between the two sources of evidence, the sediment types and argon ages, is again close to zero (Fig. 2C). In contrast to the interpretation of Owen et al. (2009), we believe that only ~13% of the Olorgesailie formation is without a record of environmental change.

The Early to Mid Pleistocene lake level record from the Olorgesailie basin reveals a relatively long episode of stability between 1.15 Ma and 0.95 Ma, which is particularly evident through a series of up to 7 m thick diatomite beds with intercalated clastic and volcanoclastic deposits (Fig. 3C; Trauth et al., 2001, 2003). Climate variability during this interval was relatively low, as pH fluctuations

between ~7.5 and 9.5 of the lake water inferred from diatom assemblages suggest (Owen et al., 2008). This episode of remarkable stability is followed by a relatively dry episode between 0.95 Ma and 0.75 Ma with predominantly subaerial conditions, before the onset of a second major lake episode between 0.75 Ma and 0.49 Ma. In contrast to the first lake episode, this lacustrine phase is characterized by rapid climate fluctuations within less than a thousand years (Owen et al., 2008).

The Ologesailie record correlates well with the Earth's eccentricity cycle modulating the amplitude of the precessional cycle (Fig. 3C). Both lake episodes correlate with maxima of the 400 kyr component of the eccentricity cycle, whereas the dry interval between 0.95 Ma and 0.75 Ma correlates with a minimum of this cycle. Most interestingly, the greater amplitude of the maximum at ~1.0 Ma seems to correlate with more stable conditions, while the second, lower maximum at ~0.6 Ma correlates with more unstable conditions. Looking at the longer, 800 kyr component of the eccentricity cycle, the transition from stable to unstable environmental conditions occurs at the descending portion of the 800 kyr component of the earth's eccentricity cycle (Fig. 3C).

4. Discussion

Our analysis of published climate time records shows that episodes of stability and instability in the environmental conditions occur on three different orbital time scales (10,000 to 1,000,000 years) during the Cenozoic.

On very long time scales of greater than one million years, changes in lakes are primarily determined by tectonics, which initially creates but also destroys lake basins. However, tectonics also affect lake conditions on shorter time scales by changing the shape and size of catchments and drainage networks (e.g., Bergner et al., 2009; Olaka et al., 2010; Trauth et al., 2010; Feibel, 2011). Furthermore, tectonics shape the morphology of lake basins and hence the sensitivity of these lakes to changes in the precipitation/evaporation balance (Olaka et al., 2010; Trauth et al., 2010). The tectonic influence on lakes is thus the first example where long-term processes can cause stable versus unstable conditions on time scales relevant for humans and other animals.

If the tectonic conditions for a lake are provided, it is mainly orbital cycles which determines the hydrological budget of the lake on time scales of 10,000 to 100,000 years (e.g., Kutzbach and Street-Perrott, 1985; Trauth et al., 2003, 2007; Kingston et al., 2007; Bergner et al., 2009; Trauth et al., 2010). The most dramatic fluctuations in humidity are caused by the 400- and 800-kyr components of the eccentricity cycle, which cause clusters of large lakes in Eastern Africa (Trauth et al., 2005, 2007). The Ologesailie record shows that the amplitude of the 400- and 800-kyr cycle affects the relative stability of the environmental conditions, with a tendency to instability in times of low amplitude (Fig. 3C). Furthermore, the Naivasha record suggests that, during an interval of maximum eccentricity between 160 ka and 50 ka, intervals of relative stability and instability alternate. At this time scale, it is the amplitude of the 100-kyr component of the eccentricity cycle that controls the amplitude of the precession cycle and hence the insolation on the African continent (Kutzbach and Street-Perrott, 1985; Trauth et al., 2003; Junginger and Trauth, 2013). Again, lower amplitudes of the 100-kyr cycle cause relative instability in the environment (Trauth et al., 2003; Fig. 3B).

If the orbital conditions (e.g., positive or negative precession during maximum eccentricity) result in highly variable lake levels, the hydrological budget of the lakes on the shorter time scales (i.e., <1000 years) is influenced by millennial scale global climate fluctuations, such as Dansgaard-Oeschger/Heinrich events including the Younger Dryas (Brown et al., 2007; Foerster et al., 2012;

Junginger and Trauth, 2013), and solar variations (Verschuren et al., 2000; Junginger et al., 2014). Interestingly, as shown by the Chew Bahir record of the Mid Holocene transition, the relation between environmental conditions and orbital forcing is highly nonlinear (Fig. 3A). After the precession minimum at ~10 ka, climate remains relatively moist despite an increase of precession from -0.018 to zero, followed by an episode of remarkable instability with at least 19 intervals of extreme aridity, recurring every 160 ± 40 years in durations of 80–20 years. Stability is reached after ~5 ka, when precession has increased above zero. Importantly, the overall transition from wet to dry at the termination of the AHP is relatively gradual, in contrast to the observation of deMenocal et al. (2000) and Tierney and deMenocal (2013; Fig. 3A).

What are the possible mechanisms for the stabilization and destabilization of environmental conditions? On very long time scales (>1,000,000 years), volcano-tectonic phenomena associated with the East African Rift System (EARS) and associated plateaus can cause both stability and instability. The formation of plateaus, as an example, has contributed very effectively to stability of the environment, as it has resulted in a blockage of moisture-bearing winds from both oceans in the West and the East and thus persistently drier conditions in Eastern Africa (Sepulchre et al., 2006; Wichura et al., 2010). On the other hand, if northern hemisphere insolation crosses a certain threshold during a precession minimum and the west-east pressure gradient increases during the July to September months, the Congo Air Boundary, currently blocked by topography, crosses the East African plateaus, bringing extra moisture from the Congo basin further to the East (Junginger and Trauth, 2013). This mechanism seems to have worked at time scales of 100 years, introducing a high level of instability if the threshold is crossed through greater insolation (Junginger et al., 2014).

Rift lakes are another factor in the development of stability and instability, as they might act as amplifiers of relatively moderate climate shifts on time scales of 1000 years (so-called amplifier lakes; Street-Perrott and Harrison, 1985; Olaka et al., 2010; Trauth et al., 2010). On the other hand, they also have a stabilizing effect by the sheer size of the water body, which reacts very slowly to changes in the moisture budget (Fig. 4). As an example, paleo-Lake Suguta in the northern Kenya Rift was about 300 m deep and 2200 km² large during the African Humid Period, while there is a 0.5–5 m deep, alkaline Lake Logipi today (Garcin et al., 2009). If there is an abrupt increase of precipitation of +25% in the 13,000 km² large catchment today, the lake would reach two thirds of the maximum lake level of 300 m not before 200 years after the climate shift, and would stabilize at the maximum lake level only after 1000 years. Gradual changes in climate would cause even longer response times of the water body. Correspondingly, an abrupt or gradual decrease of precipitation results in a delayed decline of the water level of paleo-Lake Suguta (Borchardt and Trauth, 2012; Junginger and Trauth, 2013; Fig. 4). In other words, large lakes smooth (or low-pass filter) rapid, low-amplitude variations of climate and therefore stabilize the environment.

An additional mechanism to stabilize local environmental conditions is vegetation-climate feedbacks (e.g., Jeltsch et al., 2000; Maslin, 2004; Fig. 5) wherein positive feedbacks can resist particular climate changes. For example, if an area is covered with forest, and the region starts to dry out, the vegetation recycles moisture, maintaining a level of rainfall for the forest to survive (Maslin, 2004). There is, however, a threshold at which this mechanism is not sufficient and forest is replaced by savanna. This moisture feedback does not exist with savanna; instead, the relatively dry grassland environment is maintained by recurring fires keeping trees away, similar to the activity of grazers and other factors (Jeltsch et al., 2000). Hence, the climate must get much wetter

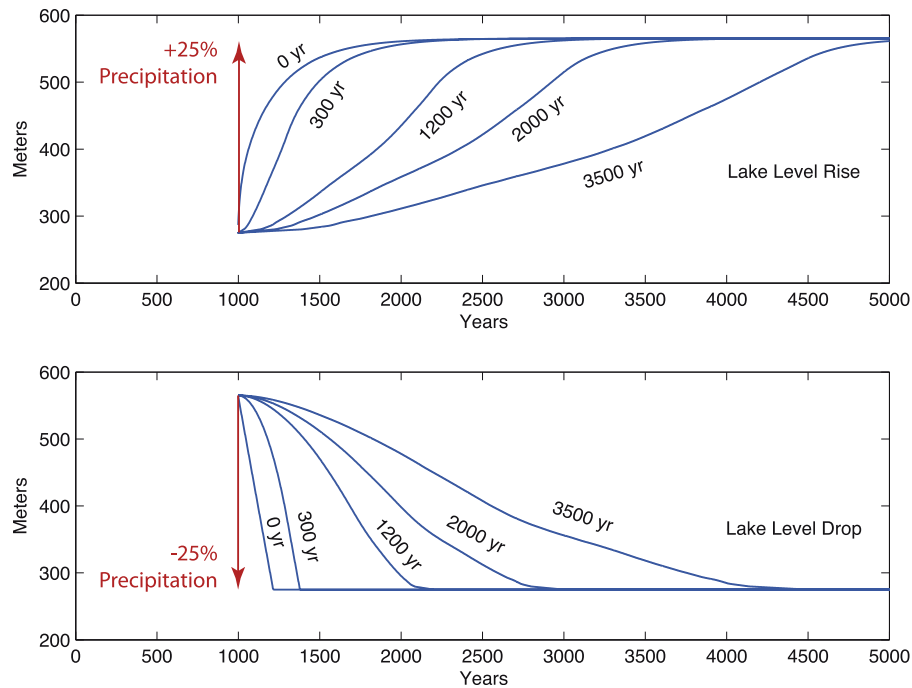


Figure 4. Stabilizing effects of lakes. Lakes have a stabilizing effect by the sheer size of the water body, which reacts very slowly to changes in the moisture budget, as lake-balance modeling suggests. If there is an abrupt increase of +25% in the 13,000 km² large catchment today, the lake would reach two thirds of the maximum lake level of 300 years not before 200 years after the climate shift, and would stabilize at the maximum lake level only after 1000 years. Gradual changes in climate would cause even longer response times of the water body (Borchardt and Trauth, 2012; Junginger and Trauth, 2013).

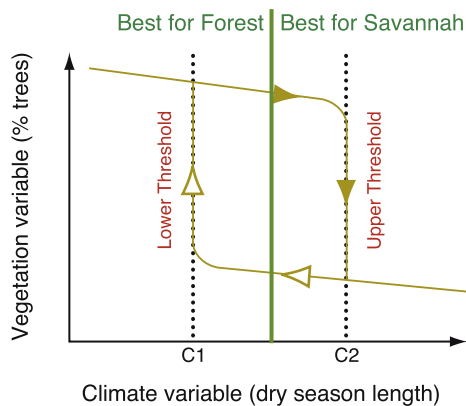


Figure 5. Bifurcation of the vegetation–climate relationship. Vegetation has a stabilizing effect on the local environment due to a positive feedback, which resists particular climate changes. For example, forests recycle moisture, maintaining a level of rainfall for the forest to survive (Maslin, 2004). This moisture feedback does not exist with savanna; instead, the relatively dry grassland environment is maintained by recurring fires keeping trees away, similar to the activity of grazers and other factors (Jeltsch et al., 2000).

before forest can recolonize that region. The interesting aspect here is the character of the transitions near the thresholds in this saddle-node bifurcated system response: how does the environment switch from one to the other stable mode? Maybe this model helps explain the remarkable instability and the occurrence of extreme droughts during the Mid Holocene wet–dry transition in the Chew Bahir basin (Fig. 3).

The observed character of transitions between stable and unstable conditions can be compared with the theoretical models proposed by Maslin and Christensen (2007) and refined by Maslin et al. (2014; Fig. 6). In their work, they present three different models of how lakes could respond to local orbital forcing. The first

model suggests that there is a relatively smooth gradual transition between periods with deep lakes and periods without lakes, which may invoke the Red Queen (Van Valen, 1973) or Turnover Pulse Hypotheses (Vrba, 1985) as possible causes of evolution (see below). The second model is a threshold model with ephemeral lakes, expanding and contracting extremely rapidly, producing the widespread, regional-scale, rapid, and extreme environmental variability required by the Variability Selection Hypothesis (Potts, 1998). The third model is characterized by extreme variability during the transitions between full to no lake conditions, which provides climate variability at a time-scale relevant to evolutionary processes. In both Models 2 and 3 human evolution could still be strongly influenced by the high-energy wet conditions or prolonged aridity (Maslin and Christensen, 2007). These models are the basis of the Pulsed Climate Variability Hypothesis (Maslin and Trauth, 2009; Trauth et al., 2010) that provides a paleoclimate framework within which to discuss the causes of early human evolution (Maslin et al., 2014). Different species or, at the very least, different emerging traits within a species could have evolved through various mechanisms, including the Turnover Pulse Hypotheses, Pulsed Climate Variability Hypothesis, or allopatric speciation.

Understanding how the East African climate switches from stability to instability is essential if we want to understand the effect of climate variation on human evolution. It is becoming apparent that different climate modes may have influenced the evolution of different species and their definitive characteristics or traits (Maslin et al., 2015). For example, the statistical modeling work of Shultz and Maslin (2013) shows that the significant brain expansion around 1.9–1.7 Ma, due to the appearance of *Homo rudolfensis*, *Homo georgicus*, and *Homo ergaster*, was associated with the emergence of ephemeral deep water lakes in almost all the East African rift basins. Maslin et al. (2014) note that although no evidence for these large brained hominins existed before 1.9 Ma, this interpretation may be limited as there is a lack of cranial capacity

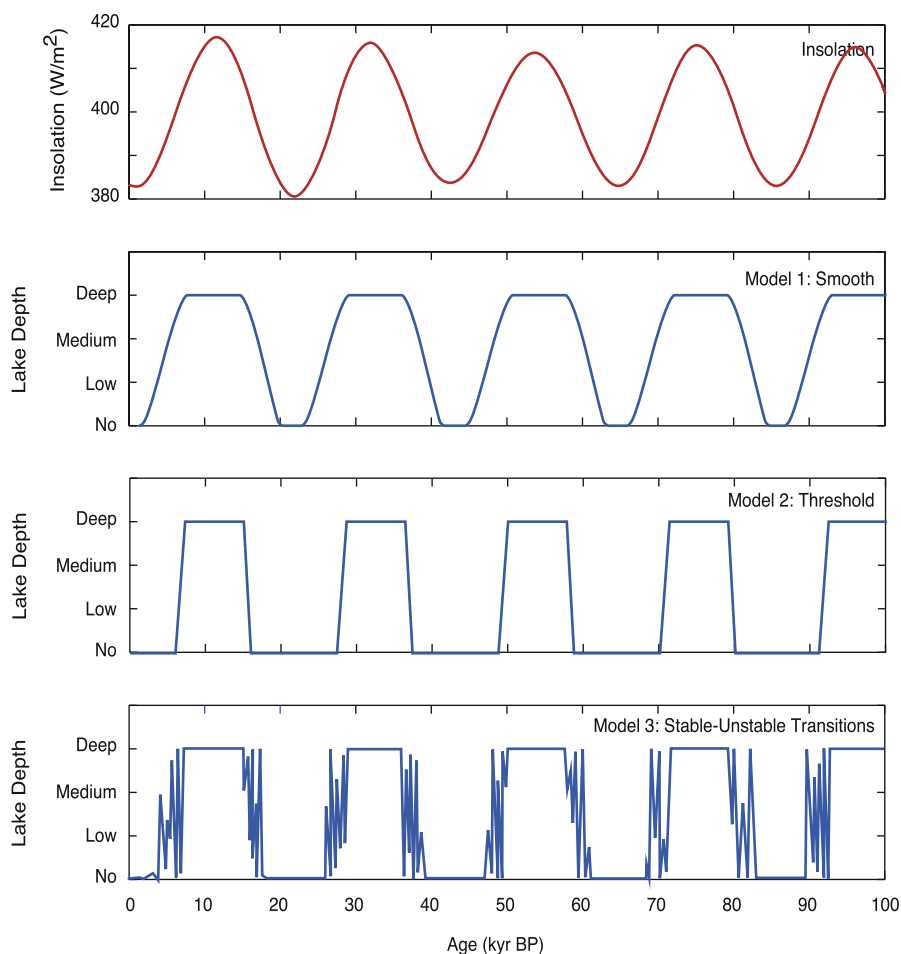


Figure 6. Models of possible environmental response to orbital forcing. The first model suggests that there is a relatively smooth gradual transition between periods with deep lakes and periods without lakes, which may invoke Red Queen (Van Valen, 1973) or Turnover Pulse Hypotheses (Vrba, 1985) as possible causes of evolution (see below). The second and third model are threshold model, with ephemeral lakes, expanding and contracting extremely rapidly, producing the widespread, regional-scale, rapid, and extreme environmental variability required by the Variability Selection Hypothesis of human evolution (Potts, 1998). The third model, however, is characterized by extreme variability during the transitions between full to no lake conditions, which implies variability influenced human evolution or again either high-energy wet conditions or prolonged aridity (Maslin and Christensen, 2007).

data between 2 Ma and 2.5 Ma. Shultz and Maslin (2013) also found that the subsequent expansion of brain capacity seems to be linked to dry stable conditions. Other characteristics that could have been forced by varying climate modes and may have been independently forced as a result of brain expansion include changes in life history (shortened inter-birth intervals, delayed development), body size, shoulder morphology allowing throwing of projectiles (Roach et al., 2013), adaptation to long distance running (Bramble and Lieberman, 2004), ecological flexibility (Hopf et al., 1993), and social behavior (Antón, 2003). At about 1.1–0.9 Ma, during the Early Mid Pleistocene Transition, environmental pressure and natural selection may have contributed to the extinction of the robust Australopithecines whose last appearance is currently dated to <1.2 Ma. *H. ergaster* survived because they were able to adapt their stone tools to a change of the environment and hence the type of food (Potts, 2013; Fig. 3A). There is also discussion about whether these changing environmental conditions could have contributed to the step like increase in brain capacity between 0.8 Ma and 1.0 Ma and the emergence of *Homo heidelbergensis* around 800 ka (Shultz et al., 2012).

The Ol Njorowa Gorge section in the Naivasha basin includes the Late Pleistocene MIS 5–4 transition, when *Homo sapiens* may have been able to expand beyond the limits of Eastern Africa into

southern Arabia, eventually during low water levels of the Red Sea and Persian Gulf for the first time when it was already wet in Eastern Africa at ~125 ka (Armitage et al., 2011). Stable environmental conditions prevailed between 150 ka and 125 ka, which may have led to an increase in the population size in Eastern Africa before the first shift towards arid conditions at ~125 ka may have caused the first expansions of this species along this southern route into Arabia (Armitage et al., 2011; Fig. 3B). The second major wave of expansion, this time through the “Nile corridor” into the Levant, occurs after ~105 ka (Niewoehner, 2001; Rightmire, 2009; Campbell and Tishkoff, 2010; Scheinfeldt et al., 2010), when climate finally got drier and unstable, according to our lake record from the Naivasha basin (Fig. 3B). This interval also coincides with increased cultural differentiation, innovation in hunting and other foraging activities, including fishing tools and the first obvious symbolic expression using preservable materials (Potts, 2013).

The Chew Bahir record ultimately shows in detail how the environment responds to gradual changes in insolation in a nonlinear, saddle-node bifurcation type transition (Fig. 3A). This high-resolution (~12 yrs) record may provide an important basis for discussion of the character and causes of the cultural transition from fishing to herding in the region (Ambrose, 1998; Marshall and Hildebrand, 2002; Scheinfeldt et al., 2010). The record clearly

shows that climate developed from wet and stable conditions until ~8.2 ka towards dry and stable conditions after ~5 ka. The intermediate interval between 8.2 ka and 5 ka is characterized by relatively wet conditions during most of the time, but punctuated by at least 19 events of extreme aridity, 20–80 years long and recurring every 160 ± 40 years, which may have made life difficult for humans living in the region. Droughts that last for several decades may have forced people to develop new technologies for food production, as documented in the archeological record.

5. Conclusions

We found episodes of stability and instability in the environmental conditions at three different orbital time scales (10,000 to 1,000,000 years) during the Cenozoic. These episodes of stability and instability may correlate with important steps in hominin speciation, brain expansion, cultural and technological innovation, and dispersal out of Africa. Hence, understanding the stability and instability of East African climate may be important if we are to increase our understanding of the key factors which may have driven human evolution.

Acknowledgments

This project was funded by grants to M.H.T. and F.S. by the German Research Foundation (DFG). The work is the result of a pilot study to the Hominin Sites and Paleolakes Drilling Project (HSPDP) in the framework of the International Continental Scientific Drilling Program (ICDP). We thank the Government of Kenya and the University of Nairobi for research permits and support. We thank A. Asrat, A.K. Behrensmeyer, I. Fer, Y. Garcin, F. Jeltsch, H. Lamb, D. Melnick, E. Odada, D. Olago, L. Olaka, R.B. Owen, R. Potts, M.R. Strecker, and R. Tiedemann for inspiring discussions. We would also like to thank H. Douglas-Dufresne and P. Ilesley of WildFrontiers Kenya, and B. Simpson and J. Roberts of TropicAir Kenya for logistical support during the helicopter expeditions to the Suguta Valley in between 2007 and 2013. The first author prefers the scientific notation of numbers when comparing the environmental changes on different time scales, such as in Figure 3. The editor Mark Teaford, however, has converted all times given in the text to the “years” (for a one-year time period, e.g. in “10,000 to 1,000,000 years” in the Discussion section) or “a” (for years ago), “ka” (for 1,000 years ago) and “Ma” (for 1,000,000 years ago) scheme. Errors in converting the times are not the responsibility of the author.

References

Ambrose, S.H., 1998. Chronology of Later Stone Age and food production in East Africa. *J. Archaeol. Sci.* 25, 377–392.

Antón, S.C., 2003. Natural history of *Homo erectus*. *Am. J. Phys. Anthropol.* 122, 126–170.

Armitage, S.J., Jasim, S.A., Marks, A.E., Parker, A.G., Usik, V.I., Uerpmann, H.P., 2011. The southern route “Out of Africa”: evidence for an early expansion of modern humans into Arabia. *Science* 331, 453–456.

Barker, P.A., Talbot, M.R., Street-Perrott, F.A., Marret, F., Scourse, J., Odada, E.O., 2004. Late Quaternary climatic variability in intertropical Africa. In: Battarbee, R.W., Gasse, F., Stickley, C.E. (Eds.), *Past Climate Variability through Europe and Africa*. Kluwer Academic Publishers, Dordrecht, pp. 117–138.

Berger, A., Loutre, M.F., 1997. Intertropical latitudes and precessional and half-precessional cycles. *Science* 278, 1476–1478.

Berger, A., Loutre, M.F., Melice, J.L., 2006. Equatorial insolation: from precession harmonics to eccentricity frequencies. *Climate of the Past* 2, 131–136.

Bergner, A.G.N., Trauth, M.H., 2004. Comparison of the hydrologic and hydrochemical evolution of Lake Naivasha (Kenya) during three highstands between 175 and 60 kyr. *Palaeogeogr. Palaeoclimatol. Palaeoecol.* 215, 17–36.

Bergner, A.G.N., Trauth, M.H., Bookhagen, B., 2003. Paleoprecipitation estimates for the Lake Naivasha basin (Kenya) during the last 175 k.y. using a lake-balance model. *Global Planet. Change* 36, 117–135.

Bergner, A.G.N., Strecker, M.R., Trauth, M.H., Deino, A., Gasse, F., Blisniuk, P., Dühnforth, M., 2009. Tectonic versus climate influences on the evolution of the lakes in the Central Kenya Rift. *Quatern. Sci. Rev.* 28, 2804–2816.

Behrensmeyer, A.K., Potts, R., Deino, A., Ditchfield, P., 2002. Olorgesailie, Kenya: a million years in the life of a rift basin. In: Renaut, R.W., Ashley, G.M. (Eds.), *Sedimentation in Continental Rifts, SEPM Special Publication*, 73, pp. 97–106.

Blaauw, M., 2010. Methods and code for ‘classical’ age-modeling of radiocarbon sequences. *Quatern. Geochronol.* 5, 512–518.

Blaauw, M., Christen, J.A., 2011. Flexible paleoclimate age-depth models using an autoregressive gamma process. *Bayesian Analysis* 6, 457–474.

Borchardt, S., Trauth, M.H., 2012. Remotely-sensed evapotranspiration estimates for an improved hydrological modeling of the early Holocene mega-lake Suguta, northern Kenya Rift. *Palaeogeogr. Palaeoclimatol. Palaeoecol.* 361–362, 14–20.

Bramble, D.M., Lieberman, D.E., 2004. Endurance running and the evolution of *Homo*. *Nature* 432, 345–352.

Bronk Ramsey, C., 1995. Radiocarbon calibration and analysis of stratigraphy: the OxCal program. *Radiocarbon* 36, 425–430.

Bronk Ramsey, C., 2008. Deposition models for chronological records. *Quatern. Sci. Rev.* 27, 42–60.

Bronk Ramsey, C., 2009a. Bayesian analysis of radiocarbon dates. *Radiocarbon* 51, 337–360.

Bronk Ramsey, C., 2009b. Dealing with outliers and offsets in radiocarbon dating. *Radiocarbon* 51, 1023–1045.

Brown, E.T., Johnson, T.C., Scholz, C.A., Cohen, A.S., King, J.W., 2007. Abrupt change in tropical African climate linked to the bipolar seesaw over the past 55,000 yrs. *Geophys. Res. Lett.* 34, L20702.

Campbell, M.C., Tishkoff, S.A., 2010. The evolution of human genetic and phenotypic variation in Africa. *Current Biology* 20, R166–R173.

Deino, A., Potts, R., 1990. Single-crystal $^{40}\text{Ar}/^{39}\text{Ar}$ dating of the Olorgesailie Formation, Southern Kenya Rift. *J. Geophys. Res.* 95, 8453–8470.

Deocampo, D.M., Behrensmeyer, A.K., Potts, R., 2010. Ultrafine clay minerals of the Pleistocene Olorgesailie Formation, Southern Kenya Rift: diagenesis and paleoenvironments of early hominins. *Clays and Clay Minerals* 58, 294–310.

deMenocal, P., Ortiz, J., Guilderson, T., Adkins, J., Sarnthein, M., Baker, L., Yarusinsky, M., 2000. Abrupt onset and termination of the African Humid Period: rapid climate responses to gradual insolation forcing. *Quaternary Science Reviews* 19, 347–361.

Feibel, C.S., 2011. A geological history of the Turkana Basin. *Evol. Anthropol.* 20, 207–216.

Foerster, V., Junginger, A., Langkamp, O., Gebru, T., Asrat, A., Umer, M., Lamb, H., Wennrich, V., Rethemeyer, J., Nowaczyk, N., Trauth, M.H., Schäbitz, F., 2012. Climatic change recorded in the sediments of the Chew Bahir basin, southern Ethiopia, during the last 45,000 yrs. *Quatern. Int.* 274, 25–37.

Foerster, V., Junginger, A., Asrat, A., Umer, M., Lamb, H.F., Weber, M., Rethemeyer, J., Frank, U., Brown, M.C., Trauth, M.H., Schäbitz, F., 2014. 46 000 years of alternating wet and dry phases on decadal to orbital timescales in the cradle of modern humans: the Chew Bahir project, southern Ethiopia. *Climate of the Past Discussions* 10, 977–1023.

Hopf, F.A., Valone, T.J., Brown, J.H., 1993. Competition theory and the structure of ecological communities. *Evol. Ecol.* 7, 142–154.

Garcin, Y., Junginger, A., Melnick, D., Olago, D.O., Strecker, M.R., Trauth, M.H., 2009. Late Pleistocene–Holocene rise and collapse of the Lake Suguta, northern Kenya Rift. *Quatern. Sci. Rev.* 28, 911–925.

Grove, M., 2013. Periods of reduced environmental variability may act as windows for hominin dispersal. *Society for American Archaeology, 78th Annual Meeting, Abstracts of Individual Presentations*, 179.

Jeltsch, F., Weber, G.E., Grimm, V., 2000. Ecological buffering mechanisms in savannas: a unifying theory of long-term tree-grass coexistence. *Plant Ecol* 161, 161–171.

Junginger, A., Trauth, M.H., 2013. Hydrological constraints of paleo-Lake Suguta in the Northern Kenya Rift during the African Humid Period (15–5 ka). *Global Planet. Change* 111, 174–188.

Junginger, A., Roller, S., Trauth, M.H., 2014. The effect of solar irradiation changes on water levels in the paleo-Lake Suguta, Northern Kenya Rift, during the late Pleistocene African Humid Period (15–5 ka). *Palaeogeogr. Palaeoclimatol. Palaeoecol.* 396, 1–16.

Kingston, J.D., Deino, A., Hill, A., Edgar, R., 2007. Astronomically forced climate change in the Kenyan Rift Valley 2.7–2.55 Ma: implications for the evolution of early hominin ecosystems. *J. Hum. Evol.* 53, 487–503.

Kutzbach, J.E., Liu, Z., 1997. Response of the African monsoon to orbital forcing and ocean feedbacks in the middle Holocene. *Science* 278, 440–443.

Kutzbach, J.E., Street-Perrott, F.A., 1985. Milankovitch forcing of fluctuations in the level of tropical lakes from 18 to 0 kyr. *Nature* 317, 130–134.

Laskar, J., Gastineau, M., Joutel, F., Robutel, P., Levrard, B., Correia, A., 2004. A long term numerical solution for the insolation quantities of Earth. *Astronomy Astrophys.* 428, 261–285.

Marshall, F., Hildebrand, E., 2002. Cattle before crops: the beginnings of food production in Africa. *J. World Prehist.* 16, 99–143.

Maslin, M.A., 2004. Ecological versus climatic thresholds. *Science* 306, 2197–2198.

Maslin, M.A., Christensen, B., 2007. Tectonics, orbital forcing, global climate change, and human evolution in Africa: introduction to the African paleoclimate special volume. *J. Hum. Evol.* 53, 443–464.

Maslin, M.A., Trauth, M.H., 2009. Plio-Pleistocene Eastern African Pulsed Climate Variability and its influence on early human evolution. In: Grine, F.E.,

- Leakey, R.E., Fleagle, J.G. (Eds.), *The First Humans—Origins of the Genus Homo*. Vertebrate Paleobiology and Paleoanthropology Series. Springer Verlag, Dordrecht, pp. 151–158.
- Maslin, M.A., Brierley, C.M., Milner, A.M., Shultz, S., Trauth, M.H., Wilson, K.E., 2014. East African climate pulses and early human evolution, commissioned review paper. *Quatern. Sci. Rev.* 101, 1–17.
- Maslin, M.A., Shultz, S., Trauth, M.H., 2015. A synthesis of the theories and concepts of early human evolution. *Philos. Trans. B* 370, 20140064.
- Potts, R., 1998. Environmental Hypotheses of Hominin Evolution. *Yearbook of Phys. Anthropol.* 41, 93–136.
- Niewoehner, W.A., 2001. Behavioral inferences from the Skhul-Qafzeh early modern human hand remains. *Proc. Natl. Acad. Sci. USA* 98, 2979–2984.
- Olaka, L.A., Odada, E.O., Trauth, M.H., Olago, D.O., 2010. The sensitivity of East African rift lakes to climate fluctuations. *J. Paleolimnol.* 44, 629–644.
- Owen, R.B., Potts, R., Behrensmeyer, A.K., Ditchfield, P., 2008. Diatomaceous sediments and environmental change in the Pleistocene Ologesailie Formation, southern Kenya Rift Valley. *Palaeogeogr. Palaeoclimatol. Palaeoecol.* 269, 17–37.
- Owen, R.B., Potts, R., Behrensmeyer, A.K., 2009. Reply to the comment on “Diatomaceous sediments and environmental change in the Pleistocene Ologesailie Formation, southern Kenya Rift Valley” by R.B. Owen, R. Potts, A.K. Behrensmeyer and P. Ditchfield. *Palaeogeogr. Palaeoclimatol. Palaeoecol.* 282, 147–148.
- Owen, R.B., Renaud, R.W., Potts, R., Behrensmeyer, A.K., 2011. Geochemical trends through time and lateral variability of diatom floras in the Pleistocene Ologesailie Formation, southern Kenya Rift Valley. *Quatern. Res.* 76, 167–179.
- Potts, R., 1996. Evolution and climate variability. *Science* 273, 922–923.
- Potts, R., 2013. Hominin evolution in settings of strong environmental variability. *Quatern. Sci. Rev.* 73, 1–13.
- Reimer, P.J., Bard, E., Bayliss, A., Beck, J.W., Blackwell, P.G., Bronk Ramsey, C., Buck, C.E., Cheng, H., Edwards, R.L., Friedrich, M., Grootes, P.M., Guilderson, T.P., Hafflidason, H., Hajdas, I., Hatté, C., Heaton, T.J., Hoffman, D.L., Hogg, A.G., Hughen, K.A., Kaiser, K.F., Kromer, B., Manning, S.W., Niu, M., Reimer, R.W., Richards, D.A., Scott, E.M., Southon, J.R., Staff, R.A., Turney, C.S.M., van der Plicht, J., 2013. IntCal13 and Marine13 Radiocarbon Age Calibration Curves 0–50,000 Years cal BP. *Radiocarbon* 55, 1869–1887.
- Rightmire, G.P., 2009. Middle and later Pleistocene hominins in Africa and South-west Asia. *Proc. Natl. Acad. Sci.* 106, 16047–16050.
- Roach, N.T., Venkadesan, N., Rainbow, M., Lieberman, D.E., 2013. Elastic energy storage in the shoulder and the evolution of high-speed throwing in *Homo*. *Nature* 498, 483–487.
- Sadler, P.M., 1999. The influence of hiatuses on sediment accumulation rates. *GeoResearch Forum* 5, 15–40.
- Scheinfeldt, L.B., Soi, S., Tishkoff, S.A., 2010. Working toward a synthesis of archaeological, linguistic, and genetic data for inferring African population history. *Proc. Natl. Acad. Sci.* 107, 8931–8938.
- Schumer, R., Jerolmack, D.J., 2009. Real and apparent changes in sediment deposition rates through time. *J. Geophys. Res.* 114, F00A06.
- Sepulchre, P., Ramstein, G., Fluteau, F., Schuster, M., Tiercelin, J.J., Brunet, M., 2006. Tectonic uplift and Eastern Africa aridification. *Science* 313, 1419–1423.
- Shultz, S., Maslin, M., 2013. Early human speciation, brain expansion and dispersal influenced by African climate pulses. *PLoS One* 8, e76750.
- Shultz, S., Nelson, E., Dunbar, R.I.M., 2012. Hominin cognitive evolution: identifying patterns and processes in the fossil and archaeological record. *Phil. Trans. R. Soc. B Biol. Sci.* 367, 2130–2140.
- Street-Perrott, F.A., Harrison, S.P., 1985. Lake levels and climate reconstruction. In: Hecht, A.D. (Ed.), *Paleoclimate Analysis and Modeling*. Wiley, New York, pp. 291–340.
- Tierney, J.E., deMenocal, P.B., 2013. Abrupt shifts in Horn of Africa hydroclimate since the last glacial maximum. *Science* 342, 843–846.
- Trauth, M.H., 2014. A new probabilistic technique to determine the best age model for complex stratigraphic sequences. *Quatern. Geochronol.* 22, 65–71.
- Trauth, M.H., Maslin, M.A., 2009. Comments on “Diatomaceous sediments and environmental change in the Pleistocene Ologesailie Formation, southern Kenya Rift” by R. Bernhart Owen, Richard Potts, Anna K. Behrensmeyer and Peter Ditchfield. *Palaeogeogr. Palaeoclimatol. Palaeoecol.* 282, 145–146.
- Trauth, M.H., Deino, A., Strecker, M.R., 2001. Response of the East African climate to orbital forcing during the Last Interglacial (130–117 kyr) and the early Last Glacial (117–60 kyr). *Geology* 29, 499–502.
- Trauth, M.H., Deino, A., Bergner, A.G.N., Strecker, M.R., 2003. Eastern African climate change and orbital forcing during the last 175 kyr. *Earth Planet. Sci. Lett.* 206, 297–313.
- Trauth, M.H., Maslin, M.A., Deino, A., Strecker, M.R., 2005. Late Cenozoic Moisture History of Eastern Africa. *Science* 309, 2051–2053.
- Trauth, M.H., Maslin, M.A., Deino, A., Strecker, M.R., Bergner, A.G.N., Dühnforth, M., 2007. High- and low-latitude forcing of Plio-Pleistocene African climate and human evolution. *J. Hum. Evol.* 53, 475–486.
- Trauth, M.H., Maslin, M.A., Deino, A., Junginger, A., Lesoloyia, M., Odada, E., Olago, D.O., Olaka, L., Strecker, M.R., Tiedemann, R., 2010. Human evolution in a variable environment: the amplifier lakes of Eastern Africa. *Quatern. Sci. Rev.* 29, 2981–3348.
- Van Valen, L., 1973. A new evolutionary law. *Evol. Theory* 1, 1–30.
- Verschuren, D., Laird, K.R., Cumming, B.F., 2000. Rainfall and drought in equatorial east Africa during the past 1,100 years. *Nature* 403, 410–413.
- Vrba, E.S., 1985. Environment and evolution: alternative causes of the temporal distribution of evolutionary events. *S. Afr. J. Sci.* 81, 229–236.
- Wichura, H., Bousquet, R., Oberhänsli, R., Strecker, M.R., Trauth, M.H., 2010. Evidence for Mid-Miocene uplift of the East African Plateau. *Geology* 38, 543–546.